Journal of Contaminant Hydrology 219 (2018) 72–85

Contents lists available at ScienceDirect

Journal of Contaminant Hydrology

journal homepage: www.elsevier.com/locate/jconhyd

The effect of freezing and thawing on water flow and MCPA leaching in partially frozen soil

Roger Holten [a,b,*], Frederik Norheim Bøe [c], Marit Almvik[a], Sheela Katuwal[d], Marianne Stenrød[a], Mats Larsbo[e], Nicholas Jarvis[e], Ole Martin Eklo[a,b]

[a] Norwegian Institute of Bioeconomy Research (NIBIO), Division of Biotechnology and Plant Health, Department of Pesticides and Natural Products Chemistry, P.O. Box 115, NO-1431 Ås, Norway
[b] Norwegian University of Life Sciences, Faculty of Bio Sciences, Department of Plant Sciences, P.O. Box 5003, N-1432 Ås, Norway
[c] Norwegian Institute of Bioeconomy Research (NIBIO), Division of Environment and Natural Resources, Department of Soil and Land Use, P.O. Box 115, NO-1431 Ås, Norway
[d] Aarhus University, Department of Agroecology, Blichers Allé 20, P.O. Box 50, DK-8830 Tjele, Denmark
[e] Swedish Agricultural University, Department of Soil and Environment, P.O. Box 7014 75007, Uppsala, Sweden

ARTICLE INFO

Keywords:
Freeze-thaw effects
Preferential flow
Macropores
Solute transport
MCPA

ABSTRACT

Limited knowledge and experimental data exist on pesticide leaching through partially frozen soil. The objective of this study was to better understand the complex processes of freezing and thawing and the effects these processes have on water flow and pesticide transport through soil. To achieve this we conducted a soil column irrigation experiment to quantify the transport of a non-reactive tracer and the herbicide MCPA in partially frozen soil. In total 40 intact topsoil and subsoil columns from two agricultural fields with contrasting soil types (silt and loam) in South-East Norway were used in this experiment. MCPA and bromide were applied on top of all columns. Half the columns were then frozen at −3 °C while the other half of the columns were stored at +4 °C. Columns were then subjected to repeated irrigation events at a rate of 5 mm artificial rainwater for 5 h at each event. Each irrigation was followed by 14-day periods of freezing or refrigeration. Percolate was collected and analysed for MCPA and bromide. The results show that nearly 100% more MCPA leached from frozen than unfrozen topsoil columns of Hov silt and Kroer loam soils. Leaching patterns of bromide and MCPA were very similar in frozen columns with high concentrations and clear peaks early in the irrigation process, and with lower concentrations leaching at later stages. Hardly any MCPA leached from unfrozen topsoil columns (0.4–0.5% of applied amount) and concentrations were very low. Bromide showed a different flow pattern indicating a more uniform advective-dispersive transport process in the unfrozen columns with higher concentrations leaching but without clear concentration peaks. This study documents that pesticides can be preferentially transported through soil macropores at relatively high concentrations in partially frozen soil. These findings indicate, that monitoring programs should include sampling during snow melt or early spring in areas were soil frost is common as this period could imply exposure peaks in groundwater or surface water.

1. Introduction

In cold climates, increased pesticide concentrations are often detected in soil leachate, drain discharge, surface runoff, and surface water bodies during freeze/thaw periods in late winter and early spring (Eklo et al., 1994; French, 1999; Riise et al., 2004; Riise et al., 2006; Siimes et al., 2006; Ulén et al., 2013). With climate change, this may become an increasingly relevant issue. For example, in the Nordic countries, climate models predict higher temperatures and more snowmelt episodes during winter and an increase in the frequency of freeze-thaw cycles of up to 38% (Hanssen-Bauer et al., 2015; Mellander et al., 2007; Lundberg et al., 2016).

However, the effects of freezing and thawing on the fate and behaviour of pesticides in soil are complex and still not well understood,

* Corresponding author at: Norwegian Institute of Bioeconomy Research (NIBIO), Division of Biotechnology and Plant Health, Department of Pesticides and Natural Products Chemistry, P.O. Box 115, NO-1431 Ås, Norway.
E-mail addresses: roger.holten@nibio.no (R. Holten), frederik.boe@nibio.no (F.N. Bøe), marit.almvik@nibio.no (M. Almvik), sheela.katuwaSl@agro.au.dk (S. Katuwal), marianne.stenrod@nibio.no (M. Stenrød), mats.larsbo@slu.se (M. Larsbo), nicholas.jarvis@slu.se (N. Jarvis), olemartin.eklo@nibio.no (O.M. Eklo).

https://doi.org/10.1016/j.jconhyd.2018.11.003
Received 23 May 2018; Received in revised form 2 November 2018; Accepted 11 November 2018
Available online 13 November 2018

so the mechanisms underlying these field observations are unclear. Soil freezing and thawing potentially influences the pathways of water flow and solute transport through soils, as well as chemical and biological processes affecting pesticide fate in the soil (Hayashi, 2013; Ireson et al., 2013).

The importance of macropores as non-equilibrium or preferential flow paths for rapid water flow and solute transport has long since been recognized (Jarvis et al., 2016; Beven and Germann, 1982). The occurrence of macropore flow can result in dramatic increases in the leaching of pesticides to groundwater and to surface water via subsurface drainage pipes (Jarvis, 2007; Flury, 1996). Macropores can be defined as pores with diameters of 0.3–0.5 mm and larger (Jarvis et al., 2017; Jarvis, 2007). These large pores have a smaller relative surface area than smaller pores and in cases where macropores dominate flow processes, solutes in flowing water can bypass bulk soil and any potential binding sites (Luxmoore et al., 1990). Examples of macropores are biopores made by earthworms and plant roots and planar fissures formed by freezing/thawing or drying/wetting. Any water present in such large pores will freeze first. As the temperature continue to decrease, water in successively smaller pores will freeze (Ireson et al., 2013). However, large macropores will often be air-filled when the soil freezes and can therefore function as effective pathways for preferential flow on thawing or if rain falls on frozen ground (Van Der Kamp et al., 2003). With subsequent freeze-thaw cycles they can become blocked with ice, which reduces the hydraulic conductivity (Ireson et al., 2013).

Models currently used in risk assessment and management do not account for the effects of freezing and thawing on pesticide leaching. Models should be tested against experimental data, hence the need to perform controlled laboratory studies or field studies to generate the data required to support the development of such a model. To date, only relatively few studies have investigated experimentally the significance of freezing and thawing for preferential transport of solutes through soil (Stadler et al., 2000; Gentry et al., 2000; Barnes and Wolfe, 2008; Wang et al., 2016; Hafsteinsdóttir et al., 2013; Wei et al., 2015). These referred studies focused mainly on the transport of tracers, nitrogen, petroleum or heavy metals. In a laboratory study, Stenrød et al. (2008) reported higher mobility of metribuzin and transport to greater depths in frozen soil compared to unfrozen soil but this study did not focus on preferential flow per se, and the results were not statistically significant. To our knowledge, no other studies of this type have been carried out specifically for pesticides.The objective of the present study was therefore to increase understanding of the effects of freezing and thawing on water flow and pesticide transport through soil. To achieve this we conducted a soil column irrigation experiment to quantify the transport of a non-reactive tracer and the herbicide MCPA in partially frozen soil. We hypothesize that columns subjected to freezing will show a higher degree of preferential transport.

2. Materials and methods

2.1. Soil sampling and characterization

Intact soil columns were sampled in May 2016 from two agricultural fields with contrasting soil types (Table 1) in South-East Norway (Kroer, 59° 38′ 37″ N 10° 49′ 58″ E; Hov 60° 12′ 45″ N 12° 1′ 58″ E). The Kroer loam have been characterized earlier by Greve et al. (1998), so no additional characterization was performed in this study. Soil characterization of the Hov silt had also been carried out earlier by the division of Survey and Statistics at NIBIO. This characterization was done according to the World Reference Base for Soil Resources, WRB (IUSS Working Group WRB, 2014). Additional information on the chemical characterization of the soils are summarized in Fig. A1 in Appendix C.

The water content of the sampled soils was neither t measured in the columns at sampling nor in the laboratory before the experiment started. This was to avoid disturbing the intact soil columns. Sampling was done in aluminium cylinders (i.d. 9.2 cm, height 20 cm). Fifty-six columns were sampled, 14 from both the topsoil (0–20 cm) and subsoil (20–40 cm) at each site. The cylinders were forced into the soil using a sledgehammer and dug out by hand, wrapped in black plastic bags and stored at ca. +4 °C. At the time of sampling, the fields were under winter wheat. Information about the use of pesticides on the sampled fields was obtained from the farmers and indicated no use of the herbicide MCPA during the last 2–3 years prior to sampling.

The soil columns were first scanned at the Department of Soil and Environment at the Swedish University of Agricultural Sciences using a high resolution industrial X-ray CT scanner (GE Phoenix v/tome/×m). The X-ray scanner had a 240 kV X-ray tube, a tungsten target (beryllium window) and a GE 16″ flat panel detector. The spatial resolution of the reconstructed 3-D images was 115 µm, with an actual resolution for feature recognition estimated to be double the pixel size (i.e. 230 µm). Radiographs collected for each soil column, in total 2000 per column, were reconstructed to 3-D images using the GE phoenix datos|x image reconstruction software. The reconstructed images were exported as 16-bit TIFF.

The X-ray images were analysed to visualize and quantify soil macropore network characteristics. The processing and analysis of the x-ray images were performed with an open source software ImageJ 1.51u (Schneider et al., 2012). Details of the image processing procedure are provided in Appendix B. Briefly, X-ray images were pre-processed for alignment, illumination correction, contrast enhancement and noise removal before applying the local adaptive thresholding method of Phansalkar et al. (2011). Using the segmented images the macroporosity ($mm^3\,mm^{-3}$), specific surface area ($mm^2\,mm^{-3}$) and the average pore thickness (mm) of the total macropore networks or the macropores pores connected throughout the soil depth, also referred to as connected macropore network, were quantified.

2.2. Chemicals

A solution of the phenoxy-acid herbicide MCPA (2-methyl-4-chlorophenoxyacetic acid, Dr. Ehrensdorfer GmbH, purity 99.5%) at a concentration of 282.6 mg L^{-1} was prepared by dissolving 70.65 mg MCPA in 250 mL acetone (VWR, Purity 99.4%). Potassium bromide (KBr) at a concentration of 11.7 g L^{-1} (7.9 g Br L^{-1}) was prepared in deionized water (Milli-Q™). MCPA is, according to the pesticide properties database (PPDB), classified as a mobile substance with typical sorption coefficients (K_f) in different soils of 0.05–1.99 mL g^{-1} (mean 0.94 mL g^{-1}). PPDB also classifies MCPA as non-persistent with a range of DT_{50} values of 7–41 days (mean 24 days) under laboratory conditions

Table 1
Selected characteristics of the studied soils.

Site	Class.[1]	Horizon, cm depth	Soil texture[2]	Clay (%)	Silt (%)	Sand (%)	pH (H_2O)	Tot. C (%)	Tot. N (%)	CEC
Kroer	Retic Stagnosol	Ap, 0–23	Loam	19.1	43.8	37.1	5.5	2.5	0.2	13.3
		Eg, 23–40	Silt loam	20.5	63.0	16.7	5.6	0.4	0.07	7.4
Hov	Dystric Fluvic Cambisol	Ap, 0–20	Silt	5.4	83.8	10.8	5.4	1.2	0.1	6.6
		Bw, 28–50	Silt	4.1	86.7	9.2	6.2	0.3	0.02	3.3

[1] WRB, 2014.
[2] USDA soil texture classification.

at 20 °C. MCPA also degrades rapidly by aqueous photolysis at pH 7 and 20 °C with a DT_{50} of 0.05 days, and even more rapidly (DT_{50} 1 h) at test conditions of pH 5–9 and 25 °C. In natural sunlight at pH 5 the DT_{50} of MCPA is 25.4 days (Lewis et al., 2016).

The MCPA metabolite 2-methyl-4-chlorophenol (2-MCP, Sigma-Aldrich, purity 99.4%) were also included in the analyses. This metabolite has been classified as slightly mobile according to PPDB, with a Koc of 882 mL g^{-1}.

A solution of artificial rainwater (Löv et al., 2017) was prepared (0.58 mg L^{-1} NaCl, 0.70 mg L^{-1} $(NH_4)_2SO_4$, 0.50 mg L^{-1} $NaNO_3$, 0.57 mg L^{-1} $CaCl_2$) and HCl (0.95 mL L^{-1} 37%) was added to obtain a pH of about 5. The rainwater was stored at about +4 °C in 20 L plastic containers.

2.3. Experimental set up

Twenty of the sampled soil columns from each of the sites Kroer and Hov, in total 40 columns, was included in the experiment. The rest of the sampled columns were excluded due to their bad condition (e.g. high content of straw in the bottom, soil was too loose and crumbled out of the columns or due to big gaps between soil and cylinder walls). The top of the soil columns was levelled to 2 cm below the rim of the top of the aluminium cylinders to ensure sufficient room for ponding during irrigation. The columns were also carefully levelled at the bottom. To achieve equal initial conditions the columns were then placed in a box of water with zero pressure potential at the bottom of the soil for a week to bring the samples close to saturation. The columns were then placed on a sand box (Eijkelkamp) where a pressure potential of −30 cm was applied at the bottom of the soil columns for a week to establish an identical initial condition for all columns, one that also ensured that all continuous macropores would be air-filled.

Five columns were randomly chosen from each soil type and depth for the freezing treatment. The remaining five columns were stored unfrozen. Analysis of Variance (ANOVA) tests performed using All Pairwise Multiple Comparison Procedures (Student-Newman-Keuls Method) in SigmaPLot (SigmaPlot for Windows Version 13.0, Systat Software, Inc.) showed no significant differences for either of the soils or depths in any of the measured pore network characteristics between the columns that underwent the freezing treatment and the unfrozen columns. All columns were then placed on fine-meshed metal sieves filled with glass beads to allow for free drainage. Thermistors were installed in the columns that were subjected to freezing to monitor the temperature during the experiment. These thermistors were installed horizontally into the center of the columns through holes in the cylinders at 7 and 14 cm depth from the soil surface The thermistors were then connected to a temperature data logger (Delta-T, Burwell - Cambridge - U.K. Accuracy ± 0.5 °C). Temperature was logged every 10 min throughout the experiment. The columns were placed on a 5 cm thick polystyrene insulation board and the column walls were covered with two layers of 2 cm thick polyethylene insulation to ensure freezing from the top and downwards.

Five mL of both the MCPA and potassium bromide (KBr) solutions were applied at the surface of each column as evenly as possible by hand using a 5 mL pipette (Finnpipette), giving rates of 2.1 kg ha^{-1} of MCPA and 59.1 kg Br^- ha^{-1}. The application rate of MCPA is an agricultural relevant rate in Norway. The insulated columns in the freezing treatment were then placed in a 1 m^3 freezing cabinet (Weisstechnik 1000SB, Weiss Technik GMBH, D-6301 Reiskirchen, Germany. Accuracy ± 0.5 °C) at −3 °C, while the unfrozen columns were kept at ca +4 °C in a refrigerated room. A temperature of −3 °C was chosen as it was considered low enough to ensure that all water in mesopores and macropores would be frozen. The top of the columns were sealed with a plastic lid and incubated at these temperatures for about four weeks. They were then subjected to repeated irrigation events with the prepared artificial rainwater, followed by 14-day periods of freezing (or refrigeration for the control columns) between irrigations. The experiment lasted for a total of 8 weeks for the silt soil (3 irrigations) and 10 weeks for the loam (4 irrigations).

The frozen columns and the unfrozen columns were transported to the irrigation room in the morning of each irrigation event. The irrigation room was at a temperature of about 5–8 °C at the start of the irrigations, but this increased to a maximum of ca. 12 °C during the day. The artificial rain water was at a temperature of about 2–4 °C at the start of each irrigation, but this increased to a maximum of about 6 °C at the end of the irrigations.

The columns were placed on top of funnels with collector flasks beneath. This setup allowed free drainage at the base of the soil columns. Irrigation water was distributed to the columns using peristaltic pumps (Autoclude model VL) adjusted to give a rate of 5 mm hr^{-1} for 5 h, resulting in a total of about 25 mm of rainwater to each column per irrigation event. Water was transferred through PVC-tubes (VWR, 4 × 6 mm) and dripped onto filter paper (Whatman Grade 1 85 mm, GE Healthcare Life Sciences) placed on the surface of the columns to ensure uniform distribution. The actual irrigation rates varied slightly between columns but there were no systematic differences between treatments, soils or depths. Preliminary tests indicated that on average the columns received 5 to 9% less water than the nominal rate. Rough calculations suggest that the total amount of irrigation water supplied to the columns during the experiment would be equivalent to ca. one pore volume.

Percolate from the soil columns during and after each irrigation was sampled in 150 mL polycarbonate bottles (Corning®, VWR) and subsamples for chemical analysis were collected manually at approximately every 25 mL until about 24 h after the start of each irrigation event. From each sub-sample, 3 mL was transferred to a 15 mL polypropylene centrifuge tube (Corning®, VWR) and stored cold (+4 °C) for later analysis of bromide. The remaining volume of leachate for each sample was stored frozen (−20 °C) in amber 60 mL glass bottles for later pesticide analysis.

Results of water and pesticides are reported as total amounts/volumes transported through the soil columns during the irrigation events (as % of the applied amounts) and as measured concentrations.

The term 5% arrival time is frequently used as an indicator of the degree of preferential flow (Koestel et al., 2011). It is usually defined as the normalized time at which 5% of the applied amount of a solute has passed through a soil column. Small values indicate a high degree of preferential transport (Larsbo et al., 2016). In our case, as the outflows are not the same for all columns even if the boundary condition is the same (a non-steady-state flow experiment), we used the 5% arrival volume for bromide to assess whether there were any differences in the strength of preferential flow between the frozen and unfrozen columns. The first 5% of the tracer mass in this instance is based on the initial applied bromide mass.

2.4. Chemical analysis

Bromide analysis was carried out using a Thermo Bromide Ion Selective Electrode (Thermo Fisher Scientific, Orion 9635BNWP) coupled to an ion meter (Mettler Toledo Seven Compact pH/Ion Meter S220) that was placed directly in the 3 mL leachate samples after addition of ionic strength adjuster (ISA, Thermo Fisher Scientific).

The concentrations of MCPA and the metabolite 2-MCP in the leachate samples were measured using LC-MS/MS (Waters Alliance 2695 LC-system coupled to a Quattro Ultima Pt triple quadropole mass spectrometer from Micromass, Manchester, UK). Leachates were filtrated with a syringe filter (PTFE 0.2 µm filter, 13 mm diameter, VWR) into vials. Leachates from the unfrozen soil columns were analysed directly, whereas the samples from the frozen columns were diluted

1 + 9 in water before analysis due to high MCPA-concentrations. 50 µL 2,4-D (Dr. Ehrensdorfer GmbH, purity 99%) was added as an internal standard to all samples at a final level of 10 ng/mL, to adjust for any variability during analysis. A 5 µL sample volume was injected, and the analytes separated on a Phenomenex Gemini C18 column (100 × 2 mm, particle diameter 3 µm) using 5 mM formic acid and methanol as mobile phases. The analytes were detected in the negative electrospray mode, with transitions *m/z* 199 > 141 and m/z 200 > 142 for MCPA and the pseudo-transition m/z 141 > 141 for 2-MCP. The MCPA metabolite 2-MCP was not detected in any of the samples. Concentrations were measured using a 5-point internal standard calibration range from 0.5–500 ng MCPA/mL. The limits of quantification were 0.125 ng MCPA/mL and 5 ng 2-MCP/mL.

After removing water for MCPA analysis, the remaining leachate was combined to make one bulk sample per column and irrigation. As 2-MCP was not detected by the method used to analyse for MCPA, selected bulk samples were concentrated and analysed for the metabolite 2-MCP.

2.5. Statistical analysis

Statistical analysis of the differences in macropore characteristics, water, bromide and MCPA transport were carried out with an analysis of variance (ANOVA) Type III test and a post-hoc pairwise Tukey test (Tukey's 'Honest Significant Difference' method) in R Commander (R Core Team, 2016). The mean total amounts of water, bromide and MCPA leached were used as response variables and soil type and treatment (frozen or unfrozen) as predictor variables (factors). Statistically significant results are reported at the 5% significance level unless otherwise stated.

3. Results

3.1. Image analysis and soil characteristics

The characteristics of the imaged macropore networks are summarized in Table 2. As was also demonstrated by Jarvis et al. (2017), the results showed that the connectivity of the macropore networks depends strongly on imaged macroporosity, with a threshold value for continuity (percolation) of ca. 4% (Fig. 1). In general, the topsoils had larger imaged porosities than the subsoils, while the loam soil at Kroer was found to have a larger imaged porosity and better connected macropore network than the silt soil at Hov (Fig. 1). In particular, the subsoil at Hov appeared to have no connected macroporosity.

3.2. Temperatures

Temperatures in the initially frozen soil columns increased quickly towards 0 °C after the start of the irrigations, but then stabilized before starting to increase again (Fig. 2). It generally took several hours before the temperatures continued to increase above 0 °C and this lag phase was longer at each irrigation. At the third irrigation of the silt, soil temperatures did not increase much above 0 °C until 27–30 h after the start of the irrigation. Another observation made, was that loam subsoil started thawing before the loam topsoil. Measurements from all thermistors at both depths (7 and 14 cm) were included in the figure but no clear difference between the two depths could be observed and the two thermistor depths have not been indicated in the figure. The data logger stopped working under the third irrigation of the Kroer loam soil columns, so no temperature curve could be obtained from this irrigation event. It took some time before the first irrigation of the Kroer loam started, hence the temperatures in the columns had risen to near 0 °C at the beginning of the irrigation.

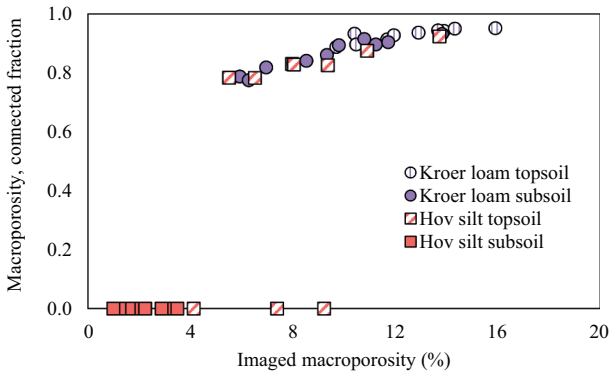

Fig. 1. The connected fraction of the macroporosity plotted as a function of imaged porosity for the Kroer loam and Hov silt topsoil and subsoil.

3.3. Infiltration and drainage

ANOVA for percolated volumes of water show that significantly larger amounts of percolation were collected from the unfrozen loam soil columns than from the frozen columns ($p < .001$) and significantly more from frozen topsoil columns than from frozen subsoil columns ($p < .05$). No significant differences were observed between the unfrozen topsoil and subsoil columns. Similar observations were made for the silt soil (Table 3).

Due to the different number of irrigations the two soils received, a direct statistical comparison of the two soil types was not performed. Nevertheless, some differences worth mentioning were observed. For example, ponding was observed on frozen columns already during the first irrigation and to a greater extent for the silt than for the loam soil. In the silt soil, ponding was even observed on unfrozen subsoil columns. In general, the extent of ponding increased in both soils for the later irrigations. In the silt, swelling or frost heave of the soil was also observed in addition to freezing of the irrigation water along the edges at the top of the soil columns, especially during the later irrigations.

Another observation made for both soil types was that when the frozen soil columns started to thaw during the irrigation, the ponded water infiltrated quickly and percolated through the columns. After thawing, 25 mL samples were collected at ca. 6–7 min intervals,

Table 2
Mean values of measured macropore network characteristics for Hov silt ($n = 20$) and Kroer loam (n = 20) soil columns. Different superscript letters denote statistically significant different results ($p < .05$), based on pairwise comparison of the samples.

Site, depth	Total macropore network			Connected macropore network		
	Mean macropor. (± SD)	Mean spec. Surface area, mm^2/mm^{-3} (± SD)	Mean thickness, mm (± SD)	Mean macropor. (± SD)	Mean spec. Surface area, mm^2/mm^{-3} (± SD)	Mean thickness, mm (± SD)
Hov silt, 0–20 cm	0.08 (0.03)^{b}	0.3 (0.09)^{b}	1.0 (0.2)^{ab}	0.05 (0.04)^{bc}	0.2 (0.2)^{bc}	0.8 (0.6)^{ab}
Hov silt, 20–40 cm	0.02 (0.01)^{c}	0.1 (0.04)^{c}	0. 9 (0.2)^{b}	0.0 (0.0)^{c}	0.0 (0.0)^{c}	0.0 (0.0)^{b}
Kroer loam, 0–20 cm	0.1 (0.02)^{a}	0.5 (0.05)^{a}	1.1 (0.1)^{a}	0.1 (0.02)^{a}	0.4 (0.06)^{a}	1.1 (0.1)^{a}
Kroer loam, 20–40 cm	0.09 (0.03)^{b}	0.4 (0.09)^{b}	1.2 (0.1)^{a}	0.08 (0.03)^{ab}	0.3 (0.1)^{ab}	1.3 (0.1)^{a}

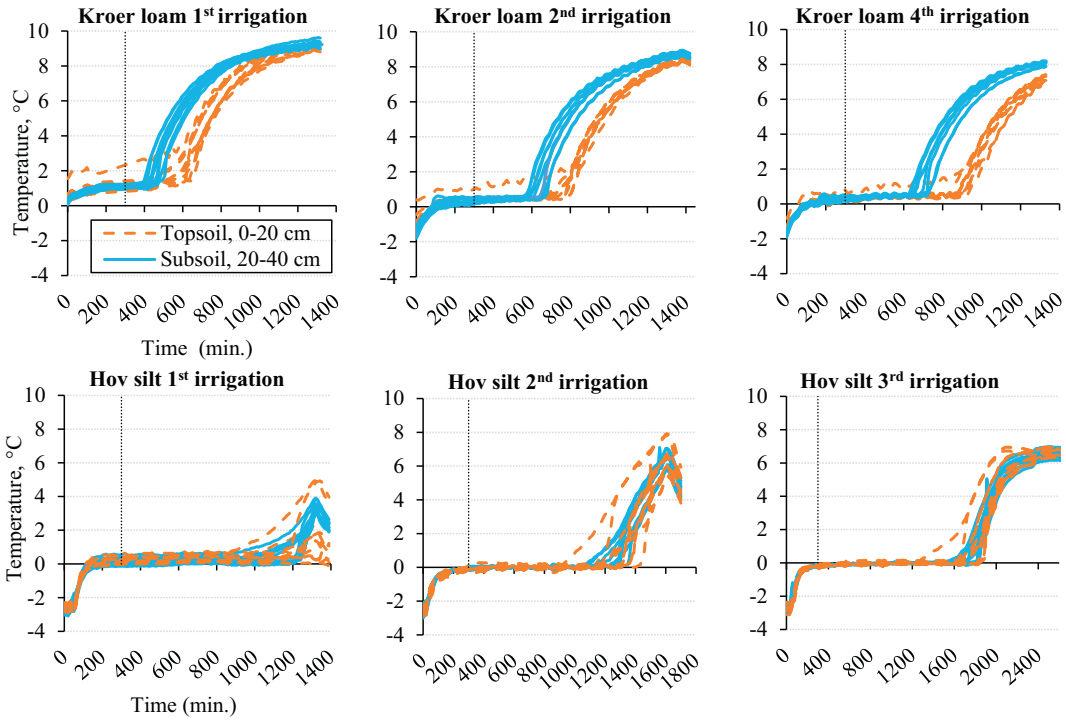

Fig. 2. Temperatures measured at 7 and 14 cm in frozen Kroer loam and Hov silt columns during three irrigation events. For the loam the curves stops at the time the columns were put back in the freezing cabinet (temperatures then started to decrease). For the silt, the temperatures continued to increase even after the columns were put back into the freezing room (around 1400 min). The end of each irrigation event (at 300 min) is symbolized with a dotted line. The same legend applies to all plots.

equivalent to flow rates of ca. 35 mm h^{-1}. This sudden infiltration was observed more often in the loam than in the silt. In contrast, the interval between each sampling in unfrozen soil was typically ca. 30 min, equivalent to a flow rate of ca. 7 mm h^{-1}.

Figs. 3 and 4 show the accumulated amount of water that percolated from frozen and unfrozen Kroer loam and Hov silt soil columns plotted against time. These figures show the constant outflow rate during irrigations of the unfrozen columns (almost equal to the inflow rate) and the rapid cessation when the irrigations stopped. This was very clear for both the loam topsoil and subsoil as well as the silt topsoil, whereas this difference was smaller for the unfrozen silt subsoil. In the frozen columns the outflow started later, especially for the later irrigations, and many of the frozen columns continued to percolate slowly a long time after irrigation ceased. During the second irrigation of the Kroer loam, some of the early samples from the frozen subsoil were lost due to leakages through the thermistor holes. The holes were re-sealed before the next irrigation. This was not believed to influence the overall results.

3.4. Bromide leaching

Following the pattern observed for the percolation of water, significantly ($p < .001$) more bromide leached from the unfrozen loam columns than from the frozen loam columns in both topsoil and subsoil (Table 3). On average, significantly more bromide leached from the unfrozen loam subsoil than the unfrozen loam topsoil ($p < .05$). In the case of the silt soil, there were no statistically significant differences between the amounts of bromide leached from frozen and unfrozen topsoil columns ($p > .05$). For subsoil on the other hand, the results were similar to what was observed for the loam.

Table 3
Total amount of water, bromide and MCPA percolated from Kroer loam soil columns during four irrigations and Hov silt soil columns during three irrigations. Different superscript letters denote statistically significant different results, based on pairwise comparison of samples from the same soil.

Soil	Soil depth (cm)	Temp. treatm. (°C)	Water		Bromide		Bromide	MCPA	
			(mm) mean (SD)	(% of applied[1])	(mg) mean (SD)	(% of applied)	5% arrival vol. mean (SD)	(µg) mean (SD)	(% of applied[2])
Kroer, loam	0–20	-3	60.2 (4.9)^{b}	60.2	14.7 (1.3)^{c}	37.4	7.5 (5.0)^{de}	346.5 (96.9)^{a}	24.5
	0–20	+4	91.2 (3.4)^{a}	91.2	22.6 (4.0)^{b}	57.5	18.0 (6.6)^{bcd}	5.0 (3.9)^{b}	0.4
	20–40	-3	47.1 (6.5)^{c}	47.1	11.1 (3.6)^{c}	28.2	3.6 (3.4)^{e}	327.9 (51.4)^{a}	23.2
	20–40	+4	87.1 (4.4)^{a}	87.1	28.3 (1.7)^{a}	72.1	7.8 (2.2)^{cde}	121.1 (97.2)^{b}	8.6
Hov, silt	0–20	-3	56.8 (6.0)^{B}	75.7	9.9 (3.5)^{AB}	25.2	5.6 (3.3)^{de}	232.2 (47.7)^{A}	16.4
	0–20	+4	70.5 (2.1)^{A}	94.0	12.3 (3.8)^{A}	31.5	35.8 (6.6)^{a}	7.5 (2.6)^{B}	0.5
	20–40	-3	39.5 (4.4)^{C}	52.7	5.1 (1.7)^{B}	13.1	20.9 (6.9)^{bc}	145.3 (58.7)^{A}	10.3
	20–40	+4	61.5 (9.0)^{AB}	82.0	11.9 (3.5)^{A}	30.4	26.2 (11.5)^{ab}	149.8 (100.4)^{A}	10.6

[1] % of nominal amount of water added.
[2] % of nominal (measured amounts in the applied pesticide solution were 102% of nominal).

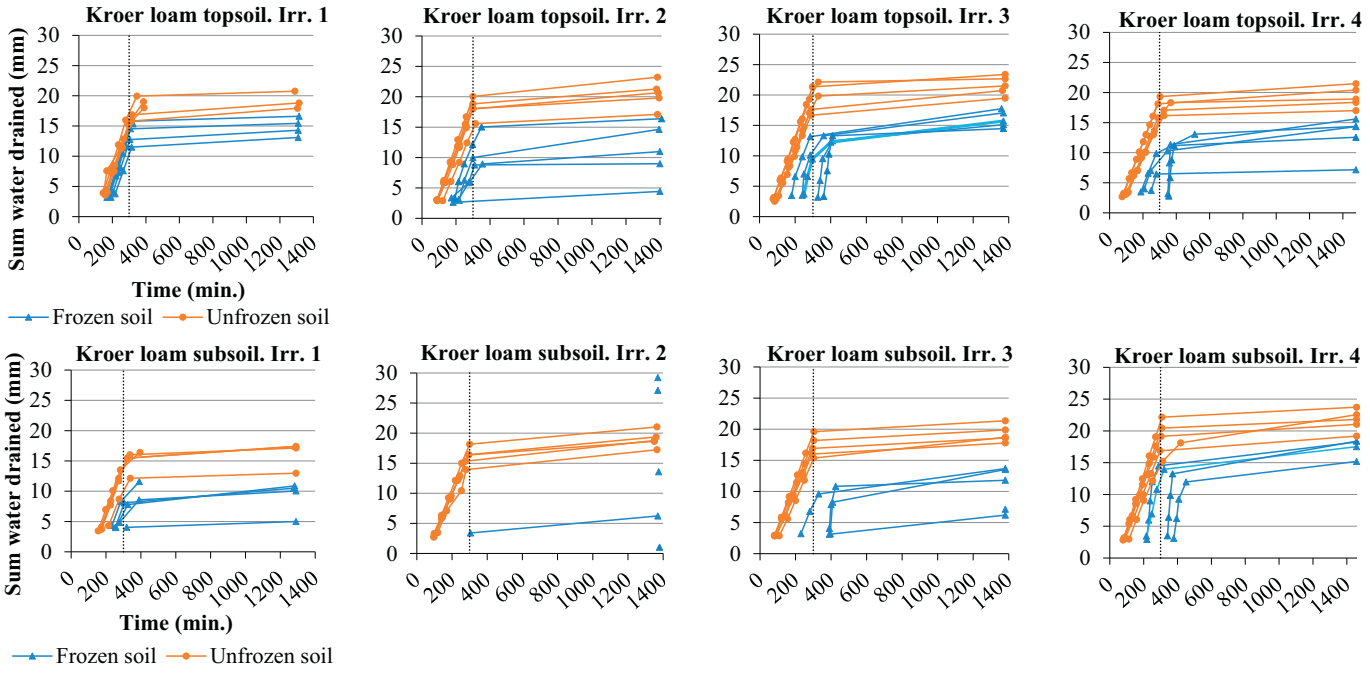

Fig. 3. The accumulated amount of water that drained from frozen and unfrozen soil columns during four irrigation events of the Kroer loam topsoil and subsoil, plotted against time. The vertical dotted line illustrates the end of the irrigations. During the second irrigation, some of the early samples from the subsoil were lost due to leakages through the thermistor holes. The same legend apply to all plots.

The leaching patterns of bromide are illustrated in Figs. 5 and 6 for typical columns from each soil and treatment combination. It was difficult to pick representative columns but the purpose was to illustrate that, for these soils and treatments, preferential flow occurred, although manifested slightly differently for different columns. Figs. 5 show evidence of strong preferential flow through the frozen topsoils of the loam columns, with the highest bromide concentrations found in the first sample of the second irrigation. Results from the other loam topsoil columns showed the same pattern albeit with some variations in the timing of the peak bromide concentrations (Fig. A1 in Appendix A). The evidence of strong preferential flow was weaker for the frozen silt topsoil columns (Fig. 6), though clearer for two of the columns (Fig. A3

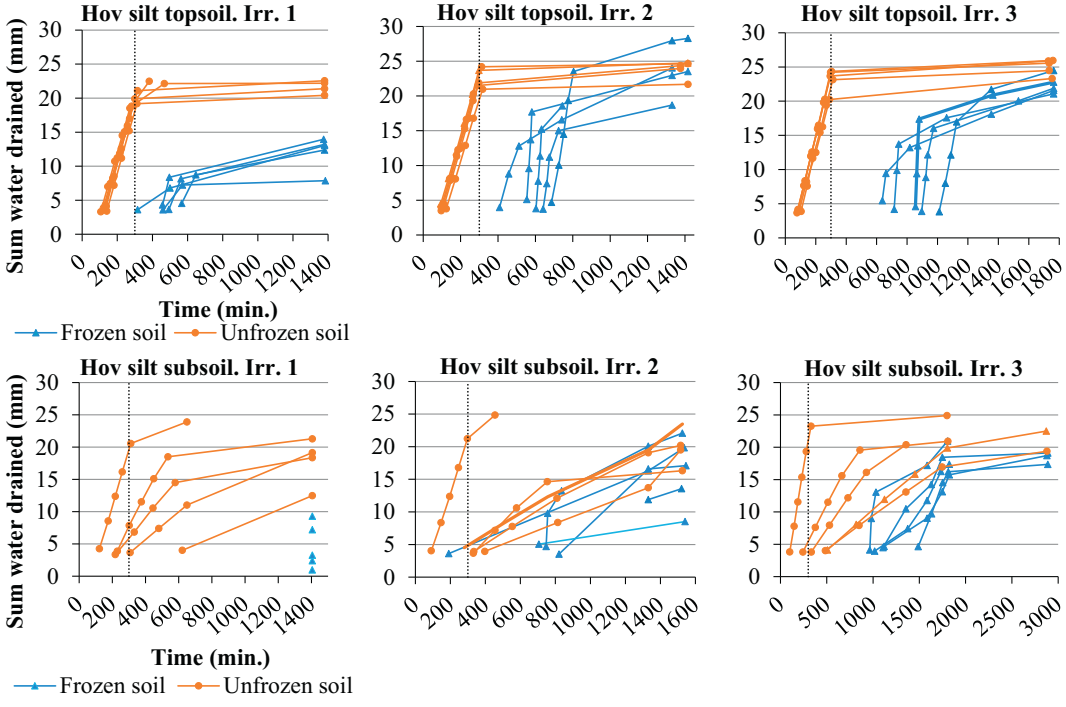

Fig. 4. The accumulated amount of water that drained from frozen and unfrozen soil columns during three irrigation events of the Hov silt topsoil and subsoil, plotted against time. The vertical dotted line illustrates the end of the irrigations. Different time scales are due to large variations in infiltration times. Only one sample was collected for each frozen subsoil column at the first irrigation due to very little percolation. The same legend apply to all plots.

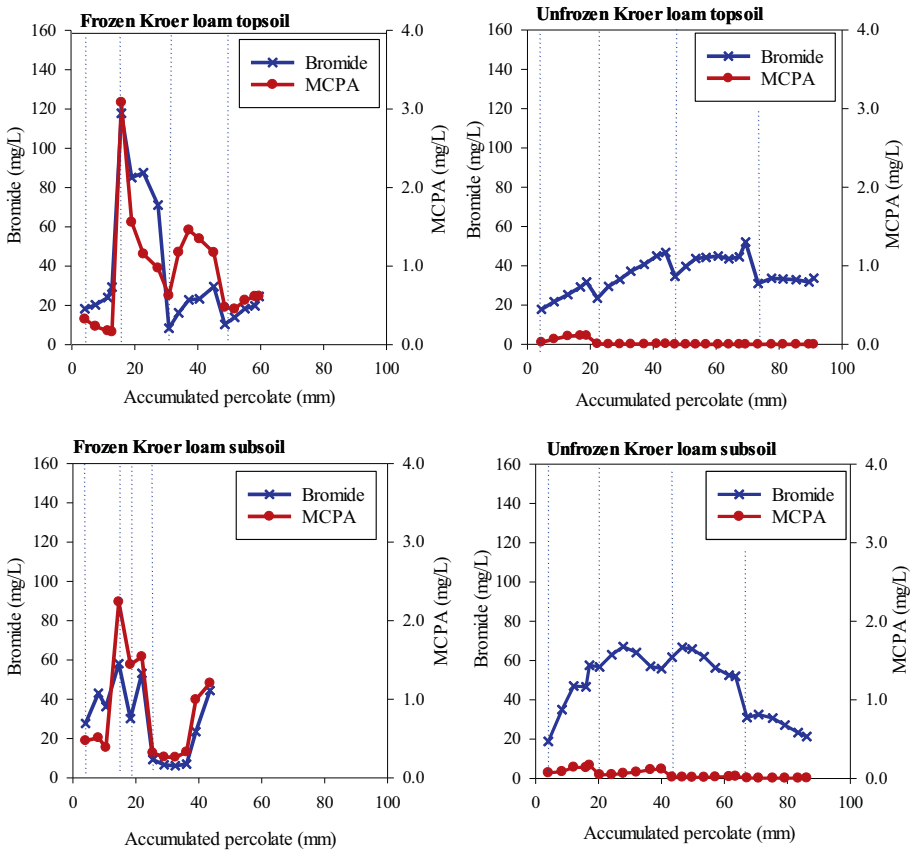

Fig. 5. Bromide and MCPA (mg L^{-1}) concentrations plotted as a function of accumulated amount of percolate (mm) for a representative soil column from frozen and unfrozen topsoil and subsoil of Kroer loam and Hov silt. Dotted lines indicate the first sampling of leachate after the onset of a new irrigation.

in Appendix A) where an early breakthrough of relatively high concentrations of bromide was observed in the first collected samples. This pattern was not equally clear for the frozen silt subsoil (Fig. 6 and Fig. A3 in Appendix A).

Contrary to the frozen soils, the leaching patterns were quite different in the unfrozen soils with smoother breakthrough curves without distinct early concentration peaks, especially evident in the loam soil (Fig. 5). Data for the other columns show the same pattern (see Appendix A).

The calculated 5% arrival volumes support the results shown above, with smaller values found for the frozen soils than unfrozen soils (Table 3). However, statistically significant differences between frozen and unfrozen columns were only found for the silt topsoil ($p < .001$). Furthermore, a statistically significant difference was found between unfrozen silt and loam columns for both topsoil and subsoil ($p < .01$), which confirms that preferential flow was generally stronger in the loam soil.

3.5. MCPA leaching

In contrast to water and bromide, significantly more MCPA leached from frozen topsoil and subsoil loam columns than from the unfrozen soils ($p < .001$, Table 3). Similar results were found for the silt topsoil, where the mean amount of MCPA leached from frozen columns was significantly larger ($p < .01$) than from the unfrozen columns. For the unfrozen silt soil, MCPA leaching was significantly larger ($p < .05$) from the subsoil than from the topsoil (Table 3).

In the frozen loam columns, the shapes of the breakthrough curves for MCPA were strikingly similar to those of bromide with peak concentrations of MCPA of ca. 2 to 3 mg L^{-1} measured in leachate by the end of the first irrigation (Fig. 5). MCPA concentrations also peaked early in the unfrozen loam columns (peaks hidden because of the scale of the plots), but the concentrations were much smaller and significantly less MCPA leached from unfrozen columns during the experiment (Fig. 5, Table 3). MCPA breakthrough curves for all loam columns are collected in Appendix A (Fig. A2).

Similar to the loam soil, most of the frozen silt topsoil columns showed early concentration peaks for MCPA, although the measured concentrations in the percolate were much smaller and the pattern was less clear than for the loam (Fig. 6, Fig. A4 in Appendix A). MCPA concentrations in leachate from the unfrozen silt topsoil columns were much smaller than for the frozen columns (Fig. 6) and hardly any MCPA leached from these columns (Table 3). Leaching losses of MCPA were similar for frozen and unfrozen silt subsoil (Table 3). The breakthrough curves of the frozen silt subsoil columns peaked at different irrigations (Fig. A 4 in Appendix A), but four of the unfrozen silt subsoil columns showed a pattern closer to the one observed for bromide leaching, i.e. smoother breakthrough curves without clear concentration peaks. One of the unfrozen silt subsoil columns differed from the others though, by showing an early concentration peak (Fig. 6). MCPA breakthrough curves for all silt columns are collected in Appendix A (Fig. A4).

A general observation made for many of the columns was the smaller concentrations of MCPA and bromide in the first sample after the start of a new irrigation. This applied especially to bromide (Fig. 5) but was also observed for MCPA (Fig. 6).

The metabolite 2-MCP was detected in some of the bulk samples

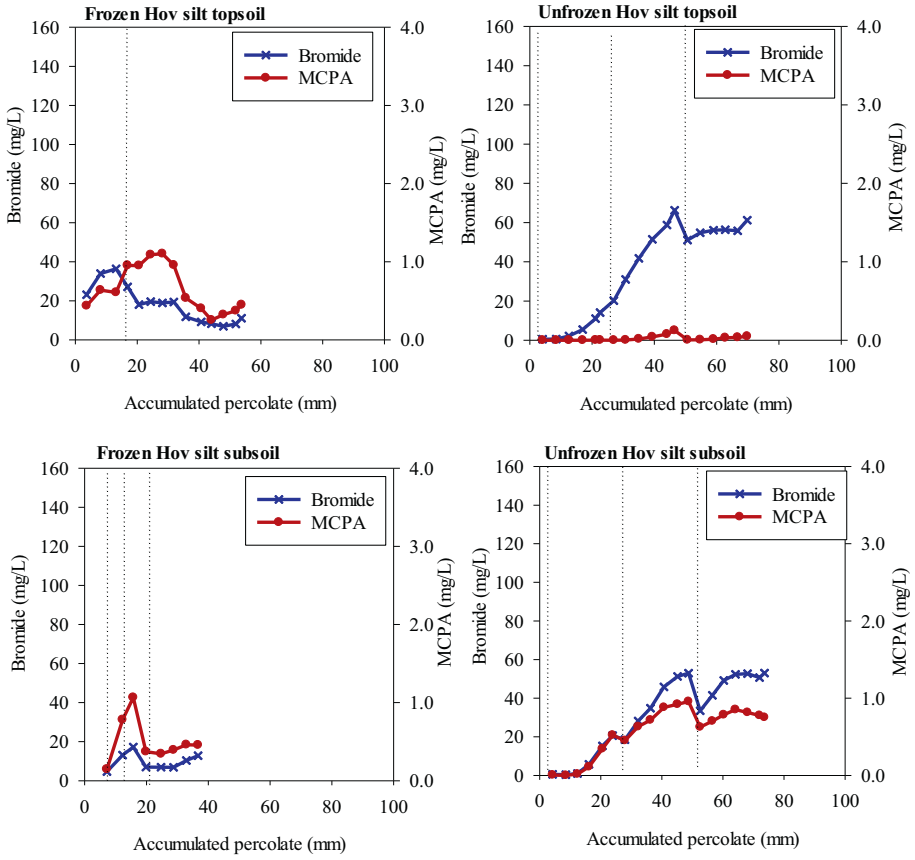

Fig. 6. Bromide and MCPA (mg L^{-1}) concentrations plotted as a function of accumulated amount of percolate (mm) for a representative soil column from from frozen and unfrozen topsoil and subsoil of Kroer loam and Hov silt. Dotted lines indicate the first sampling of leachate after the onset of a new irrigation.

from both frozen and unfrozen soil columns, both from loam and silt soils. In leachate from frozen Kroer loam topsoil columns, 2-MCP was only detected in the samples from the last irrigation at concentrations of about 0.3 µg L^{-1}. The metabolite was not detected in leachate from unfrozen loam topsoil or frozen loam subsoil. In unfrozen loam subsoil the metabolite was found in all samples from three columns at concentrations between 0.04 and 0.49 µg L^{-1} (mean 0.16 µg L^{-1}). The maximum amounts detected of the metabolite was in unfrozen Kroer loam subsoil and equalled to about 0.02% of the applied amount of MCPA. The metabolite was not detected in leachate samples from the Hov silt soil.

4. Discussion

4.1. Freeze-thaw effects on water flow and tracer transport

The observed differences in leaching patterns for bromide between frozen and unfrozen columns suggest that preferential flow through continuous macropores occurred largely in the frozen soils. The calculated lower 5% arrival volumes for frozen columns also support this conclusion (Table 3). Contrary to this, the bromide breakthrough curves from the unfrozen columns indicate a slower and more uniform advective-dispersive transport process through the whole soil matrix. The bromide breakthrough curves follow the same pattern in many of the frozen columns (Figs. 5, 6 and Appendix A), with large concentrations peaking after relatively small amounts of water had percolated through the columns followed by tailing to smaller concentrations. This applied to both loam and silt soils, although the silt did not show the same clear preferential flow pattern as the loam, especially in the subsoil, presumably because it was limited by the lack of continuity of the macropore network (Fig. 1 and Jarvis et al. (2016)). However, even for the silt soil, the 5% arrival volumes indicated stronger preferential flow for frozen soils than unfrozen soils (Table 3). The differences observed in 5% arrival volume were only statistically significant in topsoil, although the breakthrough curves indicated the same tendency for both soils.

Smaller concentrations of bromide were detected in the first percolate samples after the onset of a new irrigation than in the final samples of the previous irrigation. This could be partly explained by the fact that as soil water freezes, solutes may become concentrated in the unfrozen water in the smaller pores and as temperatures increase again, solutes may only slowly diffuse back into the mobile water in larger pores (Stähli and Stadler, 1997; Ireson et al., 2013). Thus, when the soil thaws again, the first water draining from the macropores may be relatively clean (Larsson et al., 1999).

In general, the transport patterns indicating preferential flow through macropores occurred during the earliest irrigations, when the macropores presumably were still air-filled. Later, when more water had been applied, the larger pores also became blocked by ice, resulting in reduced hydraulic conductivity and slower thawing (Ireson et al., 2013; Moghadas et al., 2016). The ponding observed on top of many columns at the initial stages of the later irrigations supports this assumption. For the frozen loam soil, ponding was first observed during the second irrigation, but some of the silt columns exhibited ponding already during the first irrigation. Hence, water content is important for how fast the thawing process occurs. In addition to the ponding, this was observed as the frozen columns both started to thaw (Fig. 2) and drain (Figs. 2-3) later at later irrigations in this experiment. These

observations were more evident for the silt than the loam. This could be explained by less pore space being available for infiltration of water and that infiltration was so slow that the increased exposure to ice caused its freezing on the way down (Moghadas et al., 2016). This could also be the reason why it took so long for the water to infiltrate the silt subsoil during and after the last irrigation (Fig. 4).

When the frozen soil columns started to thaw during the irrigations, the ponded water infiltrated quickly and percolated through the columns. After thawing, 25 mL samples were collected at ca. 6–7 min intervals, equivalent to flow rates of ca. 35 mm $h^{-}1$ being a lot faster than the fastest flow rates observed for unfrozen columns (ca. 7 mm h^{-1}). This fast infiltration was not observed for silt subsoil, being in line with the estimations of relatively high 5% arrival volume values (Table 3), indicating a little degree of preferential flow, and the smaller content of connected macropores in this soil (Fig. 1).

In addition to the different leaching patterns observed for bromide between the two treatments, significantly less amounts of bromide leached from frozen columns compared to unfrozen columns (Table 3). Brown et al. (2000) discussed that preferential flow rapidly can transport small amounts of bromide to depth, but that over a longer leaching period, preferential flow will give smaller total losses of bromide than matrix flow. This is because preferential flow interacts with only a small part of the soil and associated solute. In our case the difference observed in bromide leaching could also be due to the fact that significantly less water was collected from the frozen soil columns than the unfrozen columns. As the frozen columns thawed, one would not expect any difference in the total amount of water percolating. There were indications that the frozen columns had not finished draining after the cessation of irrigation, as a loss of water from the columns was observed while moving them before transportation between the freezing facilities and the lysimeter laboratory. Furthermore, ice was observed under the frozen columns in the freezing cabinet. Continued sampling beyond 24 h after the start of irrigation would have been desirable to sample more water from the frozen columns, but due to time constraints, this was not possible.

4.2. Freeze-thaw effects on MCPA leaching

Brown et al. (2000) argues that preferential flow seems to be the most important process for pesticide transport and that residues can be transported rapidly to deeper soil layers, while slower leaching via matrix flow not will result in larger losses over time because degradation or sorption might reduce the amounts that could leach. In this study, very little MCPA leached through the unfrozen loam and silt topsoil columns and it is possible that this could be due to faster degradation in these columns, which were maintained at higher temperatures (+ 4 °C compared with − 3 °C). The amount of MCPA retained in the soil was not measured, so the extent of degradation (and thus a complete mass balance) cannot be determined with certainty. However, the metabolite 2-MCP was detected in low amounts in some bulk leachate samples, both from frozen Kroer loam topsoil and unfrozen Kroer loam subsoil implying that some degradation did occur during the experiment. This could be due to aerobic soil degradation or more probable, due to aqueous photolysis during sampling and sample preparation since 2-MCP is a major aqueous photolysis metabolite. It is highly unlikely though that differences in degradation rates between frozen and unfrozen columns could explain the large differences observed in the leached amounts of MCPA.

The markedly larger leaching losses of MCPA from frozen topsoil columns was therefore most probably a result of much weaker sorption during transport. Sorption has been shown to be a temperature dependent process and for most compounds sorption decreases with increasing temperature (Ten Hulscher and Cornelissen, 1996; Shariff and Shareef, 2011). It could then be hypothesized that sorption would be stronger at lower temperatures. Stenrød et al. (2008) on the other hand found smaller K_d values and increased pore water concentrations for metribuzin upon release of frost in packed columns stored at − 5 °C indicating that this might not always be the case. Nevertheless, the effect of freezing on the water flow pathways is probably the most important reason for the differences observed in our experiment. Due to the fast transport through macropores, the time for adsorption of MCPA would be limited in the frozen soil columns, where flow would have been mostly restricted to the larger pores that were either initially air-filled or which drained quickly on thawing. In addition, compared to smaller pores, macropores have a small ratio of surface area to pore volume, reducing the number of available binding sites for passing solutes (Jarvis, 2007). In contrast, in the unfrozen soil with a slower and more uniform flow pattern, MCPA, although a relatively mobile substance, would be exposed to more soil surfaces and binding sites resulting in a higher degree of sorption and less MCPA being transported through the columns.

Freezing of soil can lead to frost heave, formation of ice lenses and subsequent cracking of the soil and hence an increased hydraulic conductivity (Hotineanu et al., 2015). In our case, this could have explained some of the differences observed between frozen and unfrozen columns with regards to MCPA leaching. However, less water percolated through the frozen soil columns and less bromide leached, so this was probably not a major factor. The fact that the results were quite consistent across all columns supports this conclusion. The similarity between the replicatet columns and consistent differences between the treatments also indicates that bypass of water along the side column walls was a minor problem.

Compared with the unfrozen topsoil columns, considerably more MCPA leached through the unfrozen subsoil columns (Table 3) This could have been due to significantly weaker sorption in subsoils because of smaller organic carbon contents (Hiller et al., 2010). Slower degradation in the subsoil columns during the experiment may also have been a contributing factor.

5. Conclusions

This study documents the preferential transport of MCPA and a bromide tracer through soil macropores at relatively high concentrations in partially frozen soil. Very little MCPA leached from unfrozen columns, while for bromide a more uniform advective-dispersive transport process was found. To our knowledge, these contrasting solute transport processes in frozen and unfrozen soil columns have not previously been documented experimentally.This study therefor contributes to filling an important knowledge gap. The experiment was carried out under high flow conditions in the laboratory. Nevertheless, the data collected in this study should prove useful for testing models of water flow and solute transport in partially frozen and structured soil. Our findings, together with those from other studies (Eklo et al., 1994; French, 1999; Riise et al., 2004; Riise et al., 2006; Ulén et al., 2013), also suggest that monitoring programs in climates where soil freezing is common should include sampling during snowmelt or rainfall in early spring.

Acknowledgements

This work is a part of the BIONÆR project: Innovative approaches and technologies for Integrated Pest Management (IPM) to increase sustainable food production (Smartcrop) funded by The Research Council of Norway (project no.: 244526/E50). We are grateful for the help given by Randi Bolli on the set up of the expermient and for helpful discussion of the results. I would also like to thank Jens Kværner for valuble comments during the writing process.

Appendix A

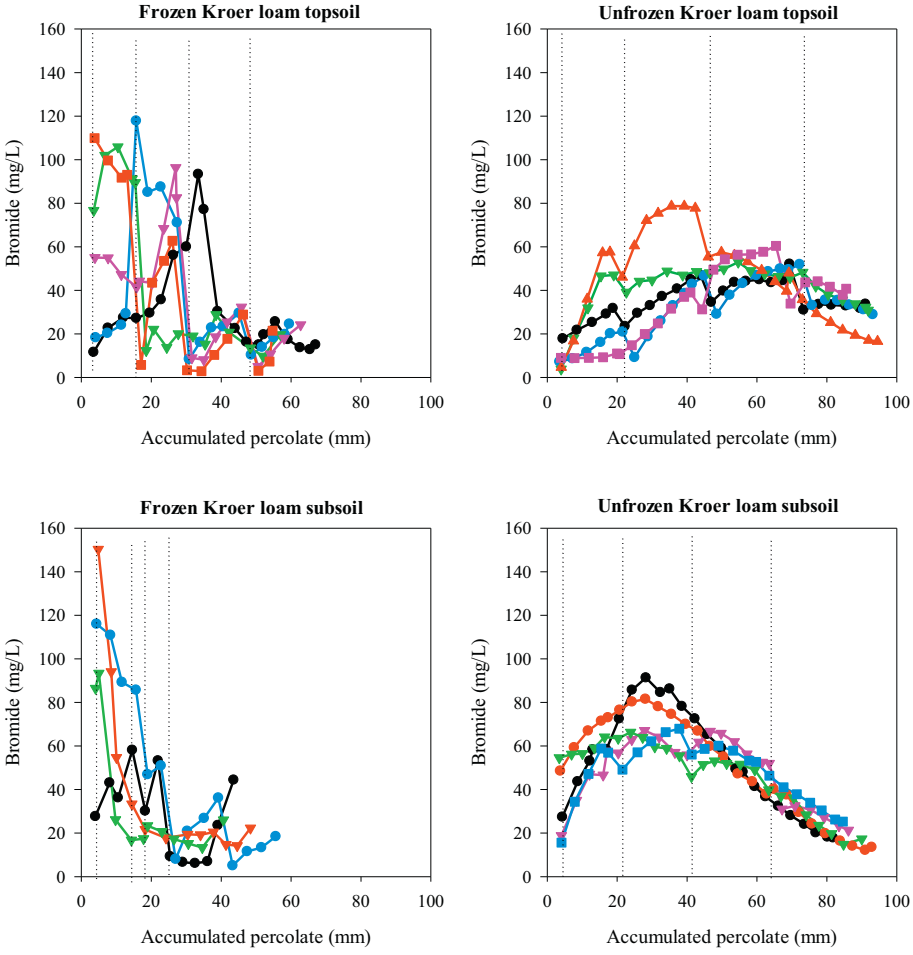

Fig. A1. Bromide (mg L^{-1}) concentrations plotted as a function of accumulated amount of percolate (mm) for all soil columns from the Kroer loam soil. Dotted lines indicate the first sampling of leachate after the start of a new irrigation. For frozen loam subsoil one of the five columns was excluded due to leakages through thermistor holes.

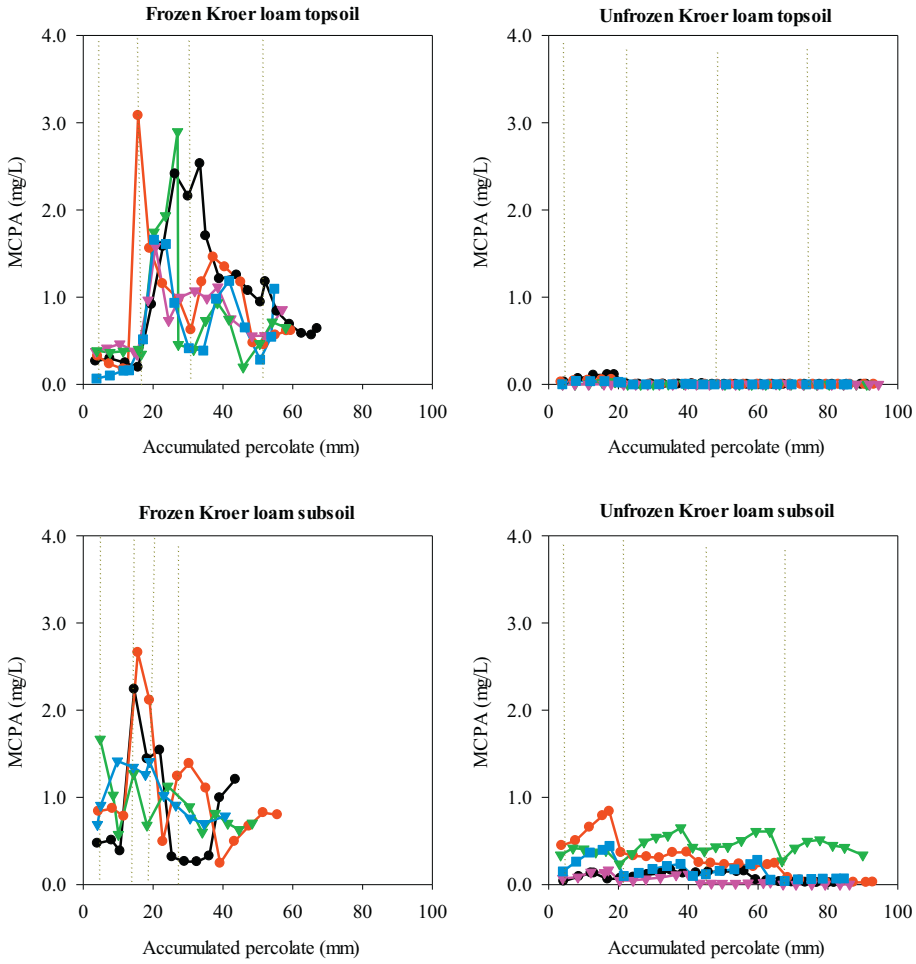

Fig. A2. MCPA ($\mu g\,L^{-1}$) concentrations plotted as a function of accumulated amount of percolate (mm) for all soil columns from the Kroer loam soil. Dotted lines indicate the first sampling of leachate after the start of a new irrigation. For frozen loam subsoil one of the five columns was excluded due to leakages through thermistor holes.

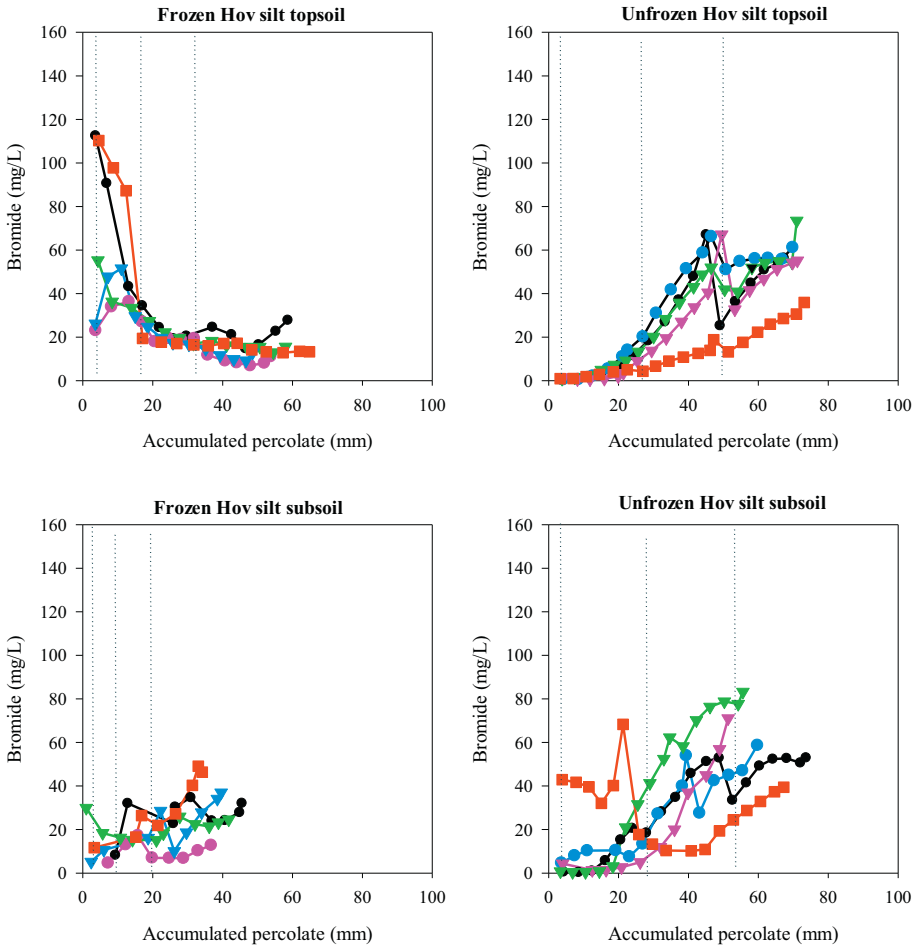

Fig. A3. Bromide (mg L^{-1}) concentrations plotted as a function of accumulated amount of percolate (mm) for all soil columns from the Hov silt soil. Dotted lines indicate the first sampling of leachate after the onset of a new irrigation.

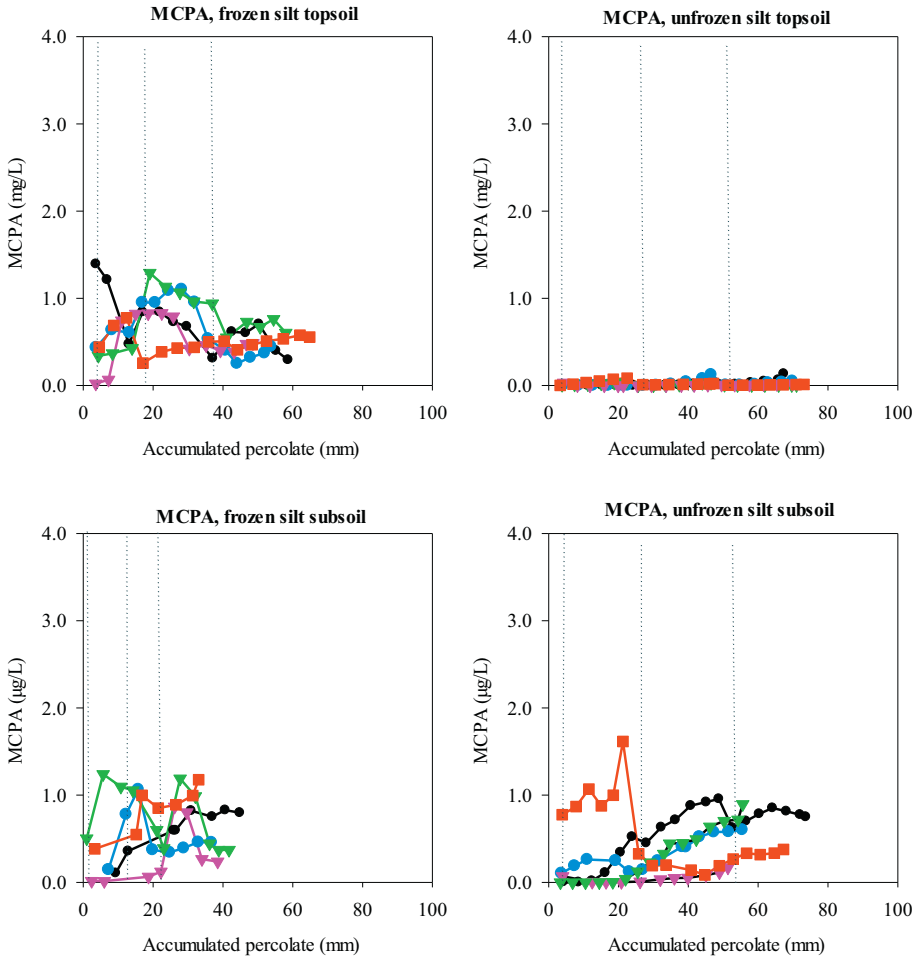

Fig. A4. MCPA (µg L^{-1}) concentrations plotted as a function of accumulated amount of percolate (mm) for all soil columns from frozen silt soil. Dotted lines indicate the first sampling of leachate after the onset of a new irrigation.

Appendix B

The reconstructed images were first corrected for the alignment to ensure that the z-axis of the soil column in the images was vertical, using the 'Untilt Stack' plugin (Cooper, 2015). Differences in illumination were observed along the z-axis of the image stack resulting possibly from the slight changes in the X-ray beam cone with scanning time. A pixel-based mathematical operation was performed for illumination correction using the mean grey value of all pixels in the 3-D image and the mean grey value of the slice containing the pixel for illumination correction. Noise in the image and poor contrast between the background and the feature of interest often interfere with the segmentation process. A 3-D median filter with a radius of 2 voxels was used for reducing the noise. The contrast between the background soil matrix and pore features was improved by normalizing the image histogram using the 'enhance contrast' algorithm (saturated pixels = 0.4%) in ImageJ. The 3-D image was cropped on the sides using a circular section to exclude the column wall, and on the top and bottom to remove the uneven and/or smeared soil surface. Segmentation of the pore features was performed using the local adaptive thresholding method of Phansalkar et al. (2011). Briefly explained, the algorithm calculates threshold value for each pixel in a slice based on the mean and standard deviation of the grey values of the neighboring pixels within a circular window specified by the user. A pixel is classified as a pore if its grey value is smaller than the calculated threshold value for that pixel. Isolated features with one pixel width in the segmented images were removed by performing an erosion operation

The segmented images were analysed for quantification of macropore properties using the 'Particle Analyzer' plugin within the 'BoneJ' plugin in ImageJ (Doube et al., 2010). The plugin labels the individual pores (set of pore voxels connected to form one cluster) and returns the measurements of various properties, selected by the user, of the labelled pores. Total macroporosity ($mm^3\,mm^{-3}$) was calculated as the volume of macropores per unit volume of soil. Macroporosity of those pores connected throughout the soil depth were referred to as connected macroporosity ($mm^3\,mm^{-3}$). The average pore thickness (mm) was calculated as the volume weighted average of the thickness of all the macropores in the analysed images.

Table A1
Cation distribution of Kroer loam and Hov silt. Data for the Kroer loam soil has been reported in Greve et al. (1998). The Hov silt has been characterized by the Division of Survey and Statistics at NIBIO according to the World Reference Base for Soil Resources, WRB (IUSS Working Group WRB, 2014).

Site	Horizon, cm depth	cmol kg^{-1}					CEC	Base sat.
		H^+	Ca	Mg	K	Na		(%)
Kroer	Ap, 0–23	4.8	7.14	0.66	0.61	0.04	13.25	64
	Eg, 23–40	2.9	3.04	0.96	0.47	0.04	7.41	61
Hov	Ap, 0–20	3.5	2.43	0.32	0.33	0.058	6.64	47
	Bw, 28–50	2.0	0.87	0.12	0.27	0.051	3.31	40

References

Barnes, D.L., Wolfe, S.M., 2008. Influence of ice on the infiltration of petroleum into frozen coarse-grained soil. Pet. Sci. Technol. 26, 856–867. https://doi.org/10.1080/10916460701824508.

Beven, K., Germann, P., 1982. Macropores and water flow in soils. Water Resour. Res. 18, 1311–1325. https://doi.org/10.1029/WR018i005p01311.

Brown, C.D., Hollis, J.M., Bettinson, R.J., Walker, A., 2000. Leaching of pesticides and a bromide tracer through lysimeters from five contrasting soils. Pest Manag. Sci. 56, 83–93. https://doi.org/10.1002/(SICI)1526-4998(200001)56:1<83::AID-PS98>3.0.CO;2-8.

Cooper, J., 2015. Untilt Stack. https://imagej.nih.gov/ij/plugins/untilt-stack/index.html.

Doube, M., Kłosowski, M.M., Arganda-Carreras, I., Cordelières, F.P., Dougherty, R.P., Jackson, J.S., Schmid, B., Hutchinson, J.R., Shefelbine, S.J., 2010. BoneJ: Free and extensible bone image analysis in ImageJ. Bone 47, 1076–1079. https://doi.org/10.1016/j.bone.2010.08.023.

Eklo, O.M., Aspmo, R., Lode, O., 1994. Runoff and leaching experiments of dichlorprop, MCPA, propiconazole, dimethoate and chlorosulfuron in outdorr lysimeters and filed catchment areas. Nor. J. Agric. Sci. 13, 7–212.

Flury, M., 1996. Experimental evidence of Transport of Pesticides through Field Soils—a Review. J. Environ. Qual. 25, 25–45. https://doi.org/10.2134/jeq1996.00472425002500010005x.

French, H.K., 1999. Transport *and degradation of deicing chemicals in a heterogenous unsaturated soil*. Doctor Scientiarum Thesis. Agricultural University of Norway ISBN: 8257503940.

Gentry, L.E., David, M.B., Smith-Starks, K.M., Kovacic, D.A., 2000. Nitrogen fertilizer and herbicide transport from tile drained fields. J. Environ. Qual. 29, 232–240. https://doi.org/10.2134/jeq2000.00472425002900010030x.

Greve, M., Helweg, A., Yli-Halla, M., Eklo, O.M., Nyborg, Å.A., Solbakken, E., Öborn, I., Stenström, J., 1998. Nordic Reference Soils. Nordic Council of Ministers 537.

Hafsteinsdóttir, E.G., White, D.A., Gore, D.B., 2013. Effects of freeze–thaw cycling on metal-phosphate formation and stability in single and multi-metal systems. Environ. Pollut. 175, 168–177. https://doi.org/10.1016/j.envpol.2013.01.007.

Hanssen-Bauer, I., Førland, E., Haddeland, I., Hisdal, H., Mayer, S., Nesje, A., Nilsen, J., Sandven, S., Sandø, A., Sorteberg, A., 2015. Klima i Norge 2100. NCCS report, Oslo, Norway. 2. pp. 1–203 (ISSN: 2387-3027).

Hayashi, M., 2013. The cold vadose zone: hydrological and ecological significance of frozen-soil processes. Vadose Zone J. 12. https://doi.org/10.2136/vzj2013.03.0064.

Hiller, E., Cernansky, S., Zemanova, L., 2010. Sorption, degradation and leaching of the phenoxyacid herbicide MCPA in two agricultural soils. Pol. J. Environ. Stud. 19, 315–321.

Hotineanu, A., Bouasker, M., Aldaood, A., Al-Mukhtar, M., 2015. Effect of freeze–thaw cycling on the mechanical properties of lime-stabilized expansive clays. Cold Reg. Sci. Technol. 119, 151–157. https://doi.org/10.1016/j.coldregions.2015.08.008.

Ireson, A.M., Van Der Kamp, G., Ferguson, G., Nachshon, U., Weather, H.S., 2013. Hydrogeological processes in seasonally frozen northern latitudes: understanding, gaps and challenges. Hydrogeol. J. 53–66. https://doi.org/10.1007/s10040-012-0916-5.

IUSS WORKING GROUP WRB, 2014. World Reference Base for Soil Resources 2014. International soil classification system for naming soils and creating legends for soil maps. In: World Soil Resources Reports No.106. FAO, Rome.

Jarvis, N.J., 2007. A review of non-equilibrium water flow and solute transport in soil macropores: principles, controlling factors and consequences for water quality. Eur. J. Soil Sci. 58, 523–546. https://doi.org/10.1111/j.1365-2389.2007.00915.x.

Jarvis, N., Koestel, J., Larsbo, M., 2016. Understanding Preferential Flow in the Vadose Zone: recent advances and Future prospects. Vadose Zone J. 15. https://doi.org/10.2136/vzj2016.09.0075.

Jarvis, N., Larsbo, M., Koestel, J., 2017. Connectivity and percolation of structural pore networks in a cultivated silt loam soil quantified by X-ray tomography. Geoderma 287, 71–79. https://doi.org/10.1016/j.geoderma.2016.06.026.

Koestel, J.K., Moeys, J., Jarvis, N.J., 2011. Evaluation of nonparametric shape measures for solute breakthrough curves. Vadose Zone J. 10, 1261–1275. https://doi.org/10.2136/vzj2011.0010.

Larsbo, M., Sandin, M., Jarvis, N., Etana, A., Kreuger, J., 2016. Surface Runoff of Pesticides from a Clay Loam Field in Sweden. J. Environ. Qual. 45, 1367–1374.

Larsson, M.H., Jarvis, N., Torstensson, G., Kasteel, R., 1999. Quantifying the impact of preferential flow on solute transport to tile drains in a sandy field soil. J. Hydrol. 215 (18). https://doi.org/10.1016/S0022-1694(98)00265-0.

Lewis, K.A., Tzilivakis, J., Warner, D.J., Green, A., 2016. An international database for pesticide risk assessments and management. Human and Ecological Risk Assessment: An International Journal 22, 1050–1064. https://doi.org/10.1080/10807039.2015.1133242.

Löv, Å., Sjöstedt, C., Larsbo, M., Persson, I., Gustafsson, J.P., Cornelis, G., Kleja, D.B., 2017. Solubility and transport of Cr(III) in a historically contaminated soil – evidence of a rapidly reacting dimeric Cr(III) organic matter complex. Chemosphere 189, 709–716. https://doi.org/10.1016/j.chemosphere.2017.09.088.

Lundberg, A., Gustafsson, D., Stumpp, C., Kløve, B., Feiccabrino, J., 2016. Spatiotemporal variations in snow and soil frost—a review of measurement techniques. Hydrology 3, 28. https://doi.org/10.3390/hydrology3030028.

Luxmoore, R.J., Jardine, P.M., Wilson, G.V., Jones, J.R., Zelazny, L.W., 1990. Physical and chemical controls of preferred path flow through a forested hillslope. Geoderma 46, 139–154. https://doi.org/10.1016/0016-7061(90)90012-X.

Mellander, P.-E., Löfvenius, M.O., Laudon, H., 2007. Climate change impact on snow and soil temperature in boreal Scots pine stands. Clim. Chang. 85, 179–193. https://doi.org/10.1007/s10584-007-9254-3.

Moghadas, S., Gustafsson, A.M., Viklander, P., Marsalek, J., Viklander, M., 2016. Laboratory study of infiltration into two frozen engineered (sandy) soils recommended for bioretention. Hydrol. Process. 30, 1251–1264. https://doi.org/10.1002/hyp.10711.

Phansalkar, N., More, S., Sabale, A., Joshi, M., 2011. Adaptive local thresholding for detection of nuclei in diversity stained cytology images. In: International Conference on Communications and Signal Processing, 10–12 Feb. 2011 2011, pp. 218–220.

R CORE TEAM, 2016. R: A Language and Environment for statistical Computing. https://www.R-project.org.

Riise, G., Lundekvam, H., Wu, Q.L., Haugen, L.E., Mulder, J., 2004. Loss of Pesticides from Agricultural Fields in SE Norway – Runoff through Surface and Drainage Water. Environ. Geochem. Health 26, 269–276. https://doi.org/10.1023/B:EGAH.0000039590.84335.d6.

Riise, G., Lundekvam, H., Haugen, L.E., Mulder, J., 2006. Suspended sediments as carriers for the fungicide propiconazole in agricultural runoff. Verhandlungen des Internationalen Verein Limnologie 1296–1300. https://doi.org/10.1080/03680770.2005.11902891.

Schneider, C.A., Rasband, W.S., Eliceiri, K.W., 2012. NIH image to ImageJ: 25 years of image analysis. Nat Meth 9, 671–675. https://doi.org/10.1038/nmeth.2089.

Shariff, R.M., Shareef, K.M., 2011. Thermodynamic adsorption of herbicides on eight agricultural soils. Int. J. Sci. Eng. Res. 2.

Siimes, K., Rämö, S., Welling, L., Nikunen, U., Laitinen, P., 2006. Comparison of the behaviour of three herbicides in a field experiment under bare soil conditions. Agric. Water Manag. 84, 53–64. https://doi.org/10.1016/j.agwat.2006.01.007.

Stadler, D., Stähli, M., Aeby, P. & Flühler, H. 2000. Dye Tracing and Image Analysis for Quantifying Water Infiltration into Frozen Soils. 64, 505–516. DOI: https://doi.org/10.2136/sssaj2000.642505x.

Stähli, M., Stadler, D., 1997. Measurement of water and solute dynamics in freezing soil columns with time domain reflectometry. J. Hydrol. 352–369. https://doi.org/10.1016/S0022-1694(96)03227-1.

Stenrød, M., Perceval, J., Benoit, P., Almvik, M., Bolli, R.I., Eklo, O.M., Sveistrup, T.E., Kværner, J., 2008. Cold climatic conditions: Effects on bioavailability and leaching of the mobile pesticide metribuzin in a silt loam soil in Norway. Cold Reg. Sci. Technol. 53, 4–15. https://doi.org/10.1016/j.coldregions.2007.06.007.

Ten Hulscher, T.E.M., Cornelissen, G., 1996. Effect of temperature on sorption equilibrium and sorption kinetics of organic micropollutants - a review. Chemosphere 32, 609–626. https://doi.org/10.1016/0045-6535(95)00345-2.

Ulén, B.M., Larsbo, M., Kreuger, J.K., Svanbäck, A., 2013. Spatial variation in herbicide leaching from a marine clay soil via subsurface drains. Pest Manag. Sci. 70, 405–414. https://doi.org/10.1002/ps.3574.

Van Der Kamp, G., Hayashi, M., Gallén, D., 2003. Comparing the hydrology of grassed and cultivated catchments in the semi-arid Canadian prairies. Hydrol. Process. 559–575. https://doi.org/10.1002/hyp.1157.

Wang, F., Ouyang, W., Hao, F., Jiao, W., Shan, Y., Lin, C., 2016. Role of freeze-thaw cycles and chlorpyrifos insecticide use on diffuse Cd loss and sediment accumulation. Sci. Rep. 6, 1–10. https://doi.org/10.1038/srep27302.

Wei, M.-L., Du, Y.-J., Reddy, K.R., Wu, H.-L., 2015. Effects of freeze-thaw on characteristics of new KMP binder stabilized Zn- and Pb-contaminated soils. Environ. Sci. Pollut. Res. 22, 19473–19484. https://doi.org/10.1007/s11356-015-5133-z.